International Civil Aviation Organisation

WORKING PAPER

The Twenty-First Meeting of the Regional Airspace Monitoring Advisory Group (RASMAG/21)

TWENTY FIRST MEETING

Bangkok, Thailand, 14-17 June 2016

Agenda Item 3: Reports from Asia/Pacific RMAs and EMAs

HORIZONTAL RISK ASSESSMENT FOR BRISBANE AND MELBOURNE FIRS

(Presented by Robert Butcher)

(Prepared by Dr Geoffrey Aldis and Dr Yuan Fang)

Summary

Traffic samples from three regions of Oceanic Control in the Brisbane and Melbourne FIRs were used to estimate lateral and longitudinal collision risk for 30 NM lateral, 30 NM longitudinal and 50 NM longitudinal separation standards. The lateral risk and the longitudinal risks were found to be well under the TLS. A speed error distribution was used which took account of the dependent nature of aircraft speeds for proximate aircraft pairs. The paper includes a description of a method for identifying passing pairs of aircraft.

1 Introduction

1.1 The Australian Airspace Monitoring Agency (AAMA), managed by the Safety and Assurance Group in Airservices Australia, performs En-route Monitoring Agency (EMA) activities for the Brisbane and Melbourne FIRs where 50 NM longitudinal and 30 NM lateral, 30 NM longitudinal separation minima have been implemented. The reduced horizontal separation minima are available for suitably equipped and PBN-approved aircraft pairs.

1.2 This monitoring report is a safety assessment for sample regions of Oceanic airspace from the Brisbane and Melbourne FIRs. Compliance with the ICAO Target Level of Safety (TLS) values is assessed for the maintenance of the reduced longitudinal and lateral separation standards.

2 Background

2.1 The ICAO-endorsed collision risk methodology described in ICAO Documents 9689 [2] and 9869 [3] is used to estimate the collision risk for each of 50 NM longitudinal, 30 NM lateral and 30 NM longitudinal separation. The risks are then compared to the TLS of 5×10^{-9} fatal accidents per flight hour (fapfh).

2.2 Use of the reduced separation standards in the Brisbane and Melbourne FIRs relies on ADS-C surveillance and CPDLC communications requirements as outlined in ICAO Document 4444 [4], such as:

- establishing ADS-C contracts with an appropriate periodic update rate for suitably approved aircraft
- establishing a lateral deviation event contract set to 5 NM
- reversion to an alternate procedural separation if an ADS-C message is overdue by 3 minutes and 6 minutes have elapsed since the controller began attempting to establish communication.

2.3 To be eligible for 50 NM longitudinal separation an aircraft must have State approval for RNP 10, RNP 4 or RNP 2. For 30 NM longitudinal or 30 NM lateral separation the approvals need to state RNP 4. Aircraft with RNP 4 and RNP 10 approvals will be equipped with CPDLC and ADS-C.

2.4 In addition, the application of the communications systems must meet RCP 240 and the surveillance system must meet RSP 180 performance (specified in [3]) in order for the reduced longitudinal separations to be applied.

3 Sample Regions of Oceanic Airspace

3.1 Figure 1 shows the Brisbane and Melbourne FIRs together with traffic in Oceanic Control Area (OCA) airspace during the period 1 March 2015 to 29 February 2016. Airservices Australia is

the air navigation service provider (ANSP) for the Brisbane and Melbourne FIRs shown. There are no organised track systems in OCA comparable to the NAT or the NOPAC.

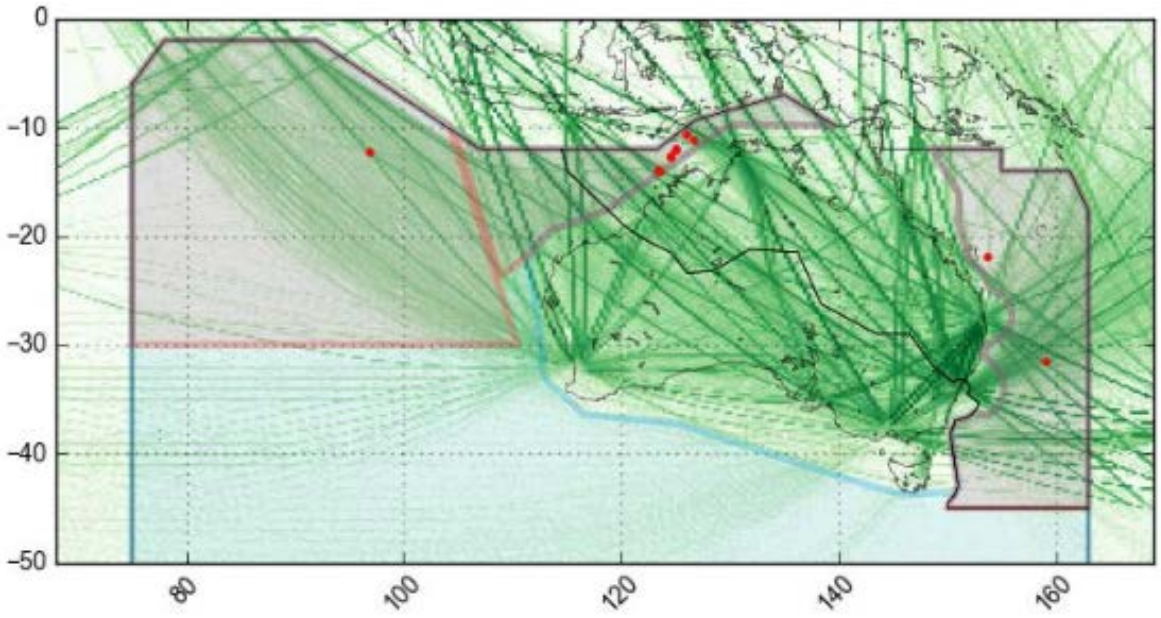

Figure 1. Flights (green) from 1 March 2015 to 29 February 2016 which reach at least FL200. Brisbane and Melbourne FIR boundaries are shown as well as the Oceanic Control Area (OCA) boundary (light blue). Latitude and longitude are shown over the coastal map. The OCA region which applies to FL245-FL600 is shown shaded. Three sample regions (pink boundaries and overshading) are left to right: WEST, NORTH and EAST. Also shown (red dots) are airports/designated landing areas which occur inside the OCA boundary at these latitudes: YPCC (Cocos Islands) in WEST, a set of offshore landing areas in NORTH, and YSEZ (Suamarez Reef seaplane base) and YLHI (Lord Howe Island) in EAST. Macquarie Island and Antarctic aerodromes are not visible in this view.

3.2 Three sample OCA regions were chosen for horizontal risk monitoring. These represent the three main traffic types. EAST and WEST were trimmed by latitude to ignore low traffic density and flex-track areas to the south. The WEST region includes UPR and flex-track traffic between the Middle East and Australia. Some crossing traffic is also included in the north-west.

3.3 The NORTH region includes traffic between Australia and Indonesia, South-East and East Asia. Traffic in NORTH follows published air-routes more than traffic in the other two regions. Two pairs of parallel one-way routes are visible between 100E and 120E. At the top boundary, the distance between ATMAL and LAMOB is 76 NM and between PUPIT and EGATU is 55 NM.

3.4 The EAST region includes traffic between Australia and New Zealand, South Pacific States and the USA. For fuel efficiency, not all traffic follows published two-way air-routes. A pair of one-way routes joining Sydney and Auckland is visible, with 52 NM between OLREL and ESKEL at the eastern FIR boundary.

4 Operators and Aircraft Types Eligible for the Reduced Horizontal Separation Minima

4.1 The flight data available for this study was comprehensive. Flights in OCA were extracted from the Airservices ODAS repository. ODAS best-estimate tracks are constructed from a merging of Flight Data Records, ADS-C, radar and ADS-B data. The tracks are available as interpolated points five seconds apart. Fields such as flight-planned communications equipment, navigation equipment, PBN approvals, ADS-C position report data and estimated track angle and ground speed are also available from ODAS.

	WEST		NORTH		EAST	
Flight-planned RNP	**%ADS**	**%nonADS**	**%ADS**	**%nonADS**	**%ADS**	**%nonADS**
RNP10 only	0.46	0.54	1.57	9.06	0.92	28.38
RNP4 only	0.08	1.54	0.78	0.23	5.81	0.09
RNP10 RNP4 only	82.09	6.30	50.89	19.02	22.01	3.97
RNP10 RNP4 RNP2	7.38	0.23	8.76	2.79	10.50	0.33
RNP10 RNP2 only	0.00	0.00	0.04	5.96	0.10	26.48
RNP4 RNP2 only	0.00	0.00	0.00	0.01	0.00	0.04
RNP2 only	0.00	0.00	0.00	0.01	0.00	0.97
None	0.69	0.69	0.23	0.64	0.05	0.37
Total ops	1301		9821		8143	
Total eligible for RNP10	1171		6093		3203	
Total eligible for RNP4	1165		5935		3120	

Table 1. Percentages of operations indicating en-route RNP approvals (RNP 10, RNP 4, RNP 2) in their flight plans, and those operations which used ADS-C. Data period is January 2016. Operations included are those which flew at FL245 or above in the WEST, NORTH or EAST oceanic sample regions. Flights were counted in the 'Total ops' of each sample region they flew in.

4.2 The row 'Total ops' in Table 1 shows the number of operations in each of the three oceanic sample regions during January 2016. These operations flew at FL245 or above in the sample regions shown in Figure 1. Some flights were counted in the 'Total ops' of more than one region.

4.3 Table 1 has rows with the flight-planned en-route RNP approvals (RNP 10, RNP 4 and RNP 2). Operations for which at least one downlink ADS-C message was received appear in a '%ADS' column, otherwise in a '%nonADS' column. The percentage for each combination of RNP approvals is shown. Percentages shown sum to 100(%) for each region.

4.4 The last two rows of Table 1 indicate the number of operations which are eligible for RNP 10 or RNP 4 separations. In each region there is little difference between the two. The rows are made of entries in an '%ADS' column which include 'RNP 10' or 'RNP 4'. Note that aircraft with an RNP 4 approval which use ADS-C are also eligible for the 50 NM longitudinal RNP 10 separation.

4.5 The percentage of operations eligible for RNP 4 separations is a:

- great majority (90%) in WEST
- majority (60%) in NORTH

- minority (38%) in EAST.

A significant amount of traffic in EAST takes place on one-way routes as RNP 2 operations.

4.6 Percentages of the most common aircraft types of RNP 4 and RNP 10 eligible aircraft are shown in Tables 2, 3 and 4. Large aircraft are common for the long trajectories in WEST. In NORTH and EAST there is more of a mixture of long-haul and short-haul aircraft. There is little difference between the RNP 4 and RNP 10 sides of each Table since most of the eligible aircraft have both RNP 4 and RNP 10 approvals.

WEST					
Eligible for RNP 4			**Eligible for RNP 10**		
Aircraft type	**% of eligible**	**cumulative %**	**Aircraft type**	**% of eligible**	**cumulative %**
B77W	36.74	36.74	B77W	36.55	36.55
A388	35.54	72.27	A388	35.35	71.90
A332	10.30	82.58	A332	10.25	82.15
A343	6.09	88.67	A343	6.15	88.30
B772	4.81	93.48	B772	4.78	93.08
B789	3.95	97.42	B789	3.93	97.01
C17	1.46	98.88	C17	1.45	98.46
A346	0.43	99.31	GLEX	0.60	99.06
B744	0.34	99.66	A346	0.43	99.49
GLEX	0.26	99.91	B744	0.34	99.83
GLF6	0.09	100.00	GLF6	0.09	99.91
			GLF5	0.09	100.00

Table 2. Aircraft type percentages for aircraft eligible for RNP 4 and RNP 10 in the WEST region.

5 Lateral Collision Risk Model

5.1 A lateral collision risk model applicable to assessing the risk, N_{ay}, of a 30 NM lateral separation standard (from Appendix 15 of ICAO Doc 9689 [2]) is:

$$N_{ay} = P_y(S_y)P_z(0)\frac{\lambda_x}{S_x}\left\{E_y(\text{same})\left[\frac{\overline{|\dot{x}|}}{2\lambda_x}+\frac{\overline{|\dot{y}(S_y)|}}{2\lambda_y}+\frac{\overline{|\dot{z}|}}{2\lambda_z}\right]+E_y(\text{opp})\left[\frac{\overline{|V|}}{\lambda_x}+\frac{\overline{|\dot{y}(S_y)|}}{2\lambda_y}+\frac{\overline{|\dot{z}|}}{2\lambda_z}\right]\right\} \quad (1)$$

where the definitions of individual parameters are given in Table 5.

5.2 The relationship between occupancy E, passing frequency N_x and number of passings b are

NORTH					
Eligible for RNP 4			**Eligible for RNP 10**		
Aircraft type	**% of eligible**	**cumulative %**	**Aircraft type**	**% of eligible**	**cumulative %**
A333	36.11	36.11	A333	36.24	36.24
B77W	15.60	51.71	B77W	15.20	51.44
A332	10.36	62.07	B788	10.47	61.91
B788	9.54	71.61	A332	10.18	72.08
A388	8.56	80.17	A388	8.35	80.44
B772	7.31	87.48	B772	7.12	87.56
B789	5.14	92.62	B789	5.01	92.57
B744	2.75	95.37	B744	2.68	95.24
B738	1.48	96.85	B738	1.44	96.68
B773	1.35	98.20	B773	1.33	98.01
MD11	0.39	98.58	GLEX	0.39	98.41
GLEX	0.34	98.92	MD11	0.38	98.79
A343	0.34	99.26	A343	0.34	99.13
B77L	0.32	99.58	B77L	0.31	99.44
C17	0.08	99.66	GLF5	0.11	99.56

Table 3. Aircraft type percentages for aircraft eligible for RNP 4 and RNP 10 in the NORTH region.

(e.g. section 5.4 of [5]):

$$\begin{aligned} N_x(\text{same}) &= \frac{\lambda_x}{S_x}\frac{\overline{|\dot{x}|}}{2\lambda_x}E_y(\text{same}) = \frac{2b_{same}}{F} \\ N_x(\text{opp}) &= \frac{\lambda_x}{S_x}\frac{\overline{|V|}}{\lambda_x}E_y(\text{opp}) = \frac{2b_{opp}}{F} \end{aligned} \tag{2}$$

where b_{same} and b_{opp} are the number of same and opposite direction aircraft passings observed in a time period during which the total aircraft flight hours are F. A factor of 2 appears with the number of passings since 2 aircraft experience each passing.

5.3 The lateral model in terms of observed number of passings is then

$$N_{ay} = \frac{2}{F}P_y(S_y)P_z(0)\left\{b_{same}\left[1+\frac{\lambda_x}{\lambda_y}\frac{\overline{|\dot{y}(S_y)|}}{\overline{|\dot{x}|}}+\frac{\lambda_x}{\lambda_z}\frac{\overline{|\dot{z}|}}{\overline{|\dot{x}|}}\right]+b_{opp}\left[1+\frac{\lambda_x}{\lambda_y}\frac{\overline{|\dot{y}(S_y)|}}{2\overline{|V|}}+\frac{\lambda_x}{\lambda_z}\frac{\overline{|\dot{z}|}}{2\overline{|V|}}\right]\right\} \tag{3}$$

6 Longitudinal Collision Risk Model

6.1 The generalized form of the longitudinal collision risk model applicable to assessing the risk, the number of accidents per flight hour, N_{ax}, associated with the 50 NM and 30 NM longitudinal separation minima is given in Appendix 1 of ICAO Doc 9689 [2]. Assuming that the aircraft pair are on the

EAST					
Eligible for RNP 4			**Eligible for RNP 10**		
Aircraft type	**% of eligible**	**cumulative %**	**Aircraft type**	**% of eligible**	**cumulative %**
B77W	17.98	17.98	B77W	17.51	17.51
A332	14.36	32.34	A332	14.24	31.75
A388	13.94	46.28	A388	13.58	45.33
B772	12.18	58.46	B772	11.86	57.20
B744	10.87	69.33	B744	10.58	67.78
B789	7.08	76.41	B789	8.80	76.58
A333	6.38	82.79	A333	6.21	82.80
B788	5.54	88.33	B788	5.43	88.23
B77L	3.91	92.24	B77L	3.81	92.04
A320	2.40	94.65	A320	2.34	94.38
MD11	1.86	96.51	MD11	1.81	96.19
B763	1.54	98.04	B763	1.50	97.69
GLEX	0.51	98.56	GLEX	0.66	98.35
C17	0.42	98.97	C17	0.41	98.75
B748	0.38	99.36	B748	0.37	99.13

Table 4. Aircraft type percentages for aircraft eligible for RNP 4 and RNP 10 in the EAST region.

same identical ground track, the risk (in fatal accidents per flight hour) during a time interval (t_0, t_1) is given by

$$N_{ax} = 2\,NP \int_{-\infty}^{\infty}\int_{-\infty}^{\infty}\int_{t_0}^{t_1} HOP(t|V_1,V_2)P_z(h_z)\left(\frac{2V_{rel}}{\pi\lambda_{xy}} + \frac{\overline{|\dot{z}|}}{2\lambda_z}\right) f_1(V_1)f_2(V_2)\,dt\,dV_1\,dV_2 \quad (4)$$

where additional parameters needed for the longitudinal collision risk model and their definitions are given in Table 6.

6.2 In equation (4) the speeds, V_1 and V_2, of the two aircraft are assumed to follow the same double exponential distribution with known means and the same scale parameter λ_v. The integrals over V_1 and V_2 with their respective probability distributions, $f_1(V_1)$ and $f_2(V_2)$, account for the variation in aircraft speed around the nominal speed.

6.3 The horizontal overlap probability term, HOP, considers the along-track and cross-track position errors of the two longitudinally separated aircraft. An equation for HOP for operations on the same ground track (track intersection angle of zero degrees) is given in Appendix 1 of ICAO Doc 9689 [2] as

$$HOP(t|V_1,V_2) = \frac{\pi\lambda_{xy}^2}{16\lambda^2}e^{-|D_x(t)|/\lambda}\left(\frac{|D_x(t)|}{\lambda}+1\right) \quad (5)$$

6.4 In equation (5) $D_x(t)$ is the distance between the aircraft pair and λ is the (same) scale parameter for the along-track and cross-track position error distributions. Along-track and cross-track deviations are modeled with a double-exponential distribution. The maximum acceptable scale parameter, λ, for a specified RNP value or a navigational accuracy value of k is $\lambda = \dfrac{-k}{\ln 0.05}$.

Parameter	Description
S_x	Nominal distance defining proximity of aircraft on adjacent parallel track to a typical aircraft
S_y	Lateral separation minimum
$P_z(0)$	Probability that two aircraft nominally on the same same flight level are in vertical overlap
$P_y(S_y)$	Probability that two aircraft nominally separated by the lateral separation minimum are in lateral overlap
λ_x	Average aircraft length
λ_y	Average aircraft wing-span (width)
λ_z	Average aircraft height with undercarriage retracted
$E_y(\text{same})$	Same-direction lateral occupancy for a pair of aircraft on the same flight level on adjacent routes separated by distance S_y
$E_y(\text{opp})$	Opposite-direction lateral occupancy for a pair of aircraft on the same flight level on adjacent routes separated by distance S_y
$N_x(\text{same})$	Same-direction longitudinal passing frequency
$N_x(\text{opp})$	Opposite-direction longitudinal passing frequency
$\overline{\lvert V \rvert}$	Average aircraft ground speed
$\overline{\lvert \dot{x} \rvert}$	Average absolute relative along-track speed between aircraft pairs
$\overline{\lvert \dot{y}(S_y) \rvert}$	Average absolute relative cross-track speed between aircraft pairs operating on tracks nominally separated by S_y
$\overline{\lvert \dot{z} \rvert}$	Average absolute relative vertical speed between aircraft pairs
b_{same}	number of same direction passings observed during a sample period
b_{opp}	number of opposite direction passings observed during a sample period
F	total aircraft flight hours observed during a sample period

Table 5. Lateral collision risk model parameters.

6.5 The application of the 30 NM longitudinal separation minimum requires aircraft to navigate to the 4 NM/95 percent accuracy criterion of RNP 4. It is known that aircraft with State Approval for RNP 4 navigate using Global Navigation Satellite Systems (GNSS). Actual aircraft performance for aircraft utilising GNSS for navigation is much better than RNP 4. To model the more accurate performance of GNSS navigation correctly, the value of k for GNSS aircraft is 0.3 NM. Risk estimate comparisons will be made between RNP 4 ($k = 4$ NM) and the assumed observed navigation performance for GNSS aircraft ($k = 0.3$ NM).

6.6 The application of the 50 NM longitudinal separation minimum requires aircraft to navigate to the 10 NM/95 percent accuracy criterion of RNP 10. However the actual navigation performance may be better than RNP 10 as aircraft eligible for the 30 MN longitudinal separation with RNP 4 are also eligible for the 50 NM longitudinal separation. Risk estimate comparisons will be made between RNP 10 ($k = 10$ NM) and the assumed observed navigation performance for GNSS aircraft ($k = 0.3$ NM).

6.7 The time integral is evaluated over $(0, T+\tau)$ where T is the ADS reporting period and τ is the controller intervention time buffer. Values of τ for 3 specific surveillance/communications scenarios (4,

10.5 and 13.5 minutes) are used as explained in [1]. The estimated longitudinal risk is then a weighted risk over the three scenarios,

$$N_{ax} = 0.95\,(0.95N_{ax}(\tau = 4) + 0.05N_{ax}(\tau = 10.5)) + 0.05N_{ax}(\tau = 13.5). \quad (6)$$

Parameter	Description
V_1	Assumed speed (knots) of aircraft 1
V_2	Assumed speed (knots) of aircraft 2
λ_{xy}	Equal to the larger of the average aircraft wingspan and length
V_{rel}	$\sqrt{V_1^2 + V_2^2 - 2V_1V_2\cos\theta}$ = relative horizontal speed between aircraft 1 and aircraft 2. Angle of zero is used for same-identical track.
NP	Number of aircraft pairs with ATC intervention per flight hour
(t_0, t_1)	Time interval over which the aircraft are considered to be longitudinally separated
$D_x(t)$	Distance between the two aircraft over the time interval (t_0, t_1)
λ_v	Scale parameter for the speed error (about the nominal speed) distribution
T	ADS periodic reporting interval
τ	Controller intervention buffer which is the time for the controller to intervene, convey instructions to the pilot and for the pilot to react and cause the aircraft to achieve a change of trajectory sufficient to ensure that a collision will be averted

Table 6. Additional parameters needed for the Longitudinal CRM.

7 Operational Errors

7.1 Airservices' safety reporting database, CIRRIS, was searched for horizontal occurrence reports which may have impacted on airspace risk. A scrutiny group assessed the reports for one month (Feb 2016). There were no risk-bearing Longitudinal events. Large lateral deviations (LLD) were included in the table below if their magnitude was at least 15 NM. Table 7 shows the assessment of the reports which were used to estimate the parameter α and then the CRM lateral overlap probability $P_y(30)$ in each region.

Date	Region	Occurrence Type	Magnitude	Code
20160212	NORTH	Lateral	22 NM	C4,W
20160221	WEST	Lateral	16 NM	C4
20160225	NORTH	Lateral	31 NM	C4
20160225	NORTH	Lateral	20 NM	B4
-	EAST	Lateral	-	-

Table 7. Reported horizontal safety occurrences assessed as risk-bearing from the month of February 2016. The final row is an unspecified entry included to allow a risk value to be calculated for EAST. Codes are: B4 = Poor centre to centre coordination; C4 = Pilot fails to follow ATC clearance; W = Weather event.

8 Parameters for the Collision Risk Models

8.1 The flight data available was aircraft flight data records (FDR) and best-estimate Airservices ODAS flight tracks. The ODAS tracks were constructed by merging FDR, ADS-C, radar and ADS-B position data and interpolated to standardised 5 second intervals. Interpolated data was sampled at 30 second intervals for this study. In OCA, flight tracks were mostly based on ADS-C position reports, FDR and occasionally ADS-B data. For aircraft not using ADS-C the flight tracks were formed from interpolation of FDR with some ADS-B. Data is therefore of high quality, particularly for aircraft eligible for the reduced separation standards.

8.2 Aircraft dimension parameters were derived from January 2016. The number of passings was estimated from all OCA traffic (including non-eligible aircraft to be conservative) for the four months November 2015 to February 2016. Aircraft speeds were estimated from aircraft in the observed passings. Operational errors were assessed from only the month of February 2016.

8.1 Aircraft dimensions: λ_x, λ_y, λ_z, λ_{xy}

8.1.1 Aircraft eligible for the reduced separation standards during January 2016 contributed to the proportion-of-tracks-by-aircraft-type weighted mean values. Only the main contributors are shown in Tables 2, 3 and 4, but all eligible aircraft types observed were used for Table 8.

	RNP 4			RNP 10		
Sample region	**Length (NM)**	**Width (NM)**	**Height (NM)**	**Length (NM)**	**Width (NM)**	**Height (NM)**
WEST	0.038245	0.036326	0.010852	0.038146	0.036234	0.010822
NORTH	0.035333	0.033264	0.009631	0.035263	0.033209	0.009608
EAST	0.035638	0.033661	0.009996	0.035521	0.033562	0.009958

Table 8. Eligible-aircraft-type-weighted mean estimates of aircraft length λ_x, wingspan λ_y, height λ_z and diameter λ_{xy}. Diameter estimates are the larger of the length and wingspan estimates in each region and choice of RNP. Data was from January 2016.

8.1.2 λ_{xy} were estimated as the maximum of the length and width values in each region and RNP category in Table 8.

8.2 Aircraft speeds: $\overline{|V|}$, $\overline{|\dot{x}|}$, V_1, V_2, V_{rel}

8.2.1 Table 9 shows the speed parameters estimated from aircraft involved in passings during November 2015-February 2016. These were used in the lateral CRM (3).

8.2.2 Parameters V_1, V_2 and V_{rel} were used in the longitudinal CRM (4). Calculations involved V_1 and V_2 sampled from double exponential speed distributions with mean speeds set to 480 knots and scale parameter $\lambda_v = 2.5$ as discussed soon. For each V_1, V_2 pair a value of V_{rel} was calculated according to the formula in Table 6 which for same identical track $\theta = 0$ reduces to $V_{rel} = |V_1 - V_2|$.

Region	$\overline{\lvert V \rvert}$ (knots)	$\overline{\lvert \dot{x} \rvert}$ (knots)
WEST	486.93	12.0
NORTH	468.54	26.54
EAST	458.29	13.63

Table 9. Aircraft speed parameters based on opposite-direction passings (mean aircraft speed $\overline{|V|}$) and same-direction passings (mean speed difference $\overline{|\dot{x}|}$). Flight track data was for the period 1 November 2015 to 29 February 2016.

8.3 Vertical overlap probability $P_z(0)$

8.3.1 The probability that two aircraft nominally at the same flight level are in vertical overlap, $P_z(0)$, is also used in RVSM risk assessment. Almost all the aircraft in the three Australian oceanic samples will be RVSM-approved. These aircraft hold their flight level accurately and the current AAMA value used for RVSM risk assessment, $P_z(0) = 0.55$ is preferred to the ([1] Appendix H NAT) value of 0.48. For this year's horizontal risk assessment $P_z(0) = 0.55$ was used.

8.4 Position errors, lateral overlap probability $P_y(S_y)$

8.4.1 Typical and atypical aircraft position errors enter the RNP 4 lateral risk model (3) through the lateral overlap probability $P_y(S_y)$ where $S_y = 30$ NM. $P_y(S_y)$ incorporates the effect of operational error as observed in the safety reporting of losses of planned separation. Specifically, the rate of Large Lateral Deviations (LLD) contributes through a parameter α. The use of position errors by the longitudinal risk model (4) is explained after the lateral.

8.4.2 A Double-Double Exponential (DDE) model of lateral deviations which includes typical and atypical error is given by

$$f(y; \alpha, \lambda_1, \lambda_2) = \frac{1-\alpha}{2\lambda_1} e^{-\frac{|y|}{2\lambda_1}} + \frac{\alpha}{2\lambda_2} e^{-\frac{|y|}{2\lambda_2}} \tag{7}$$

where f is the probability density function, y is a value of the lateral deviation random variable, α is the proportion of atypical error and λ_1 and λ_2 are scale parameters for the component Double Exponential (DE) distributions.

8.4.3 The first DE density in the weighted average (7) is the 'core' term for lateral error due to normal operations. Its scale parameter λ_1 is given by the RNP 4 lateral containment condition of 95% within ± 4 NM of the nominal track. For a DE distribution,

$$\lambda_1 = \frac{-k}{\ln 0.05} \tag{8}$$

where $k = 4$ is the required navigation performance.

8.4.4 The second scale parameter $\lambda_2 = 30$ NM is conservatively set to provide a DE distribution with mean at the parallel track spacing of 30 NM. Estimation of the weighting parameter α is discussed during the aircraft passing section.

8.4.5 The lateral overlap probability $P_y(S_y)$ is estimated as the convolution of two distributions of type (7), one centred on $y = 0$ and the other on $y = 30$ NM. The wingspan λ_y is also used to define an overlap region. Using the formulae for equal DDE distributions in the case $\lambda_y < 30$ NM from [6]

$$P_y(S;\lambda_1,\lambda_2,w,\alpha) = (1-\alpha)^2 g(\lambda_1,S,w) + 2\alpha(1-\alpha)h(\lambda_1,\lambda_2,S,w) + \alpha^2 g(\lambda_2,S,w) \quad (9)$$

$$g(\lambda,S,w) = \frac{e^{-\frac{S}{\lambda}}}{2\lambda}\left((S+2\lambda)\sinh\frac{w}{\lambda} - w\cosh\frac{w}{\lambda}\right) \quad (10)$$

$$h(\lambda_1,\lambda_2,S,w) = \frac{1}{\lambda_2^2-\lambda_1^2}\left(\lambda_2^2 e^{-\frac{S}{\lambda_2}}\sinh\frac{w}{\lambda_2} - \lambda_1^2 e^{-\frac{S}{\lambda_1}}\sinh\frac{w}{\lambda_1}\right) \quad (11)$$

where $S = S_y = 30$ and $w = \lambda_y$.

8.4.6 Table 10 shows the values used to estimate P_y and the derived estimates. Parameter α is obtained here as the number of LLDs during February/number of OCA flights during February.

Region	Risk bearing LLDs	Flights/day	α	$P_y(S_y = 30)$
WEST	1	41.744	8.261×10^{-4}	7.37×10^{-7}
NORTH	3	298.64	2.595×10^{-4}	2.12×10^{-7}
EAST	1*	240.96	1.431×10^{-4}	1.18×10^{-7}

Table 10. The number of risk-bearing LLDs during February 2016, flights per day and derived parameters α and $P_y(S_y = 30)$ for each region. *no LLDs were observed for EAST in the single-month of reports. An unspecified LLD appears here to enable a more conservative risk estimate.

8.4.7 Position errors enter the longitudinal risk model (4) through the λ parameter in (5). As is usual, RNP typical aircraft cross- and along-track position errors are assumed to have the same double-exponential distribution. For RNP 4 the scale parameter λ is related to the 95% performance $k = 4$ NM by $\lambda = -k/\ln 0.05 = 1.335$ NM. For RNP 10 it is $\lambda = 3.338$ NM. A stricter comparison case with GNSS aircraft tracking firmly on the nominal track with 'Observed Navigational Performance' ONP = 0.3 NM has $\lambda = 0.100$ NM.

8.5 Number of passings, total flight hours: b_{same}, b_{opp}, F

8.5.1 The number of passings was used in preference to occupancy due to the detailed track data available. The ODAS (Operational Data Analysis Suite) tracks are interpolated at standardised 5 second intervals. Each ODAS track is a best estimate to the true track and is obtained by merging FDR, ADS-C, radar and ADS-B position data.

8.5.2 Track angle (bearing) is available in the ODAS track data. This makes an analysis of longitudinal and lateral separation possible for a pair of aircraft. Passings can be identified by a change in sign of longitudinal separation.

8.5.3 Figure 2 shows a pair of aircraft on the surface of a sphere before, at and after a longitudinal passing. The reference aircraft A is faster than the target aircraft B. The longitudinal and lateral separation of B from the track of A can be calculated using the points C_1, C_2 and C_3 at which the great circles AC and BC intersect at a right angle. In Figure 2, the signed distance C_1A_1 is defined arbitrarily as

the positive longitudinal separation, and C_1B_1 as the positive lateral separation. At the second time, B_2 is abeam A_2. The longitudinal separation is zero and the lateral separation is C_2B_2. At the third time, aircraft A has passed aircraft B. The longitudinal separation C_3A_3 is negative and the lateral separation C_3B_3 is still positive.

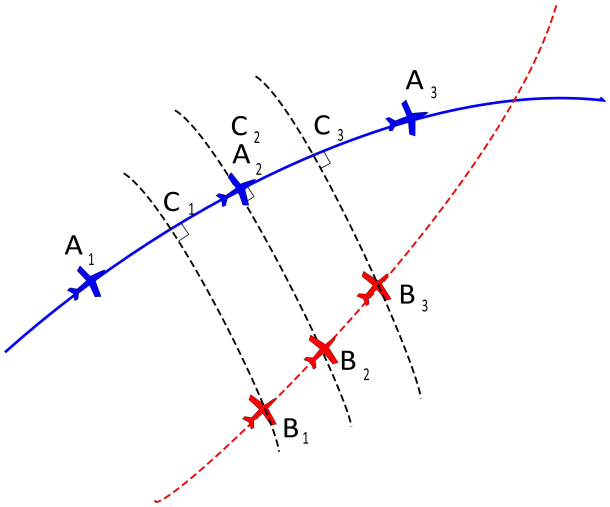

Figure 2. Diagram of an aircraft A passing another aircraft B on the surface of a spherical Earth. Longitudinal and lateral separations can be defined in terms of the intersections of great circles and the distances CA and CB as described in the text. C points are chosen as being on the great circle of aircraft A's instantaneous track, with a right angle to the great circle between C and B.

8.5.4 The algorithm used to detect passings in a given OCA region is:

- identify all tracks which enter the region during the sample period. Tracks contain at least the following fields at each time: flight identifier, latitude, longitude, altitude, time and track angle
- collect these tracks and truncate each to between the first entry time and the last exit time. Also make an index for the tracks with fields: unique identifier, entry time, exit time. Note that aircraft enter and leave the OCA region through FL245 as well as the boundaries in Figure 1
- sort the index by entry time
- loop over the first to second-last aircraft in the index, using each as the 'reference aircraft'
- find all aircraft pairs of each reference aircraft by passing forwards in the index with 'target aircraft' until the next target aircraft enters the region *after* the reference aircraft leaves. Summarise each pair by the aircraft identifiers, the start and end track line numbers of each aircraft and the start time and end time (that both aircraft are together in the region). The line numbers are used to 'zip' the tracks together over the duration of the pair
- study the proximity of each pair. For example, filter coarsely by removing pairs which do not satisfy a minimum difference in latitude, longitude and flight level over their duration. Filter finely by first finding longitudinal separation, lateral separation and flight level difference at each time. Then a passing is identified between a change of sign of longitudinal separation if the lateral separation and flight level difference are within acceptable bounds

- repeat the previous two steps with the next reference aircraft.

8.5.5 A lot (or most) of the OCA traffic occurs off published routes. Aircraft are often able to optimise their trajectories to increase fuel efficiency over the large distances and to avoid weather events. The few one-way route pairs are laterally separated by over 50 NM.

8.5.6 The lateral risk results will be conservative. Few aircraft pairs are laterally separated by the minimum 30 NM RNP 4 separation standard. In this study passings are accepted if the lateral separation at passing is less than 80 NM and the flight level difference is less than 700 feet. Passings are classified as 'same-direction' for track intersection angles up to 45 degrees, as 'opposite-direction' down to 135 degrees, and the remainder are 'crossing tracks'. To simplify the working with a more conservative risk estimate, all OCA aircraft were regarded as RNP 4 when estimating passings and calculating the lateral risk.

8.5.7 In Figure 3 a reference aircraft is at A and a target aircraft is at B. Great circle arcs are defined by: joining the aircraft at A and B; by the instantaneous trajectory at A projected back to C, which is the position abeam the target aircraft; and the great circle between C and B.

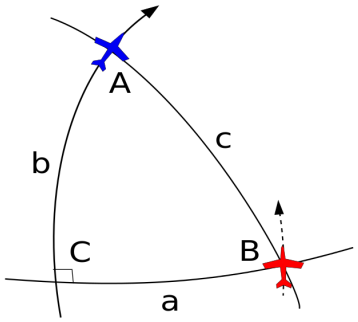

Figure 3. A pair of aircraft and the spherical triangle used to calculate longitudinal and lateral separation. A, B and C are vertices or angles (depending on context) and a, b and c are signed distances (NM) of the opposite sides. Great circles join A, B and C. The position of A and the reference aircraft's track angle define the great circle passing through A and C, where C is the point abeam the second aircraft (angle C is a right angle). b (here negative) is longitudinal separation, a (positive) is lateral separation, and c is the distance between the two aircraft. The great circle of the instantaneous trajectory of the aircraft at B is shown dashed. The angle between the track angles of the aircraft at A and B leads to an intersection angle for the two aircraft tracks.

8.5.8 Spherical trigonometry including Napier's Rules for right spherical triangles are used to calculate signed distances a (lateral separation) and b (longitudinal separation). The example has a negative longitudinal separation and a positive lateral separation. The key formulae (with A and c calculated and with C a right angle) are:

$$a = R \arcsin(\sin(A) \sin(\frac{c}{R})) \quad (12)$$

$$b = R \arctan(\cos(A) \tan(\frac{c}{R})) \quad (13)$$

where R is the radius of the spherical Earth (NM).

8.5.9 A degenerate triangle occurs if A is an integer multiple of $\pi/2$ radians, but then the distance between A and B is simply a lateral or a longitudinal separation.

8.5.10 The number of same and opposite direction passings observed in the OCA track data during 1 November 2015 to 29 February 2016 are shown in Table 11.

Region	b_{same}	b_{opp}	F **(flight hours)**
WEST	4	27	14408
NORTH	11	141	21602
EAST	14	409	33100

Table 11. Number of same-direction, opposite-direction passings and flight hours observed in the OCA track data during 1 November 2015 to 29 February 2016.

8.6 Other kinetic term parameters: $\overline{|\dot{y}(S_y)|}$, $\overline{|\dot{z}|}$

8.6.1 $\overline{|\dot{y}(S_y)|}$ is the average relative lateral speed of two aircraft nominally on parallel tracks separated by S_y. The finite time between position reports in oceanic airspace allows an aircraft to drift laterally without detection. This term was treated in Appendix H of [1] as due to a waypoint insertion error, in which an aircraft followed an incorrect track in order to arrive at an incorrect waypoint on an adjacent track, where $S_y = 30$ NM is the track spacing. A waypoint insertion error is an operational error well-known in track systems like the NAT, but it is hard to see how it applies to the three sample regions of this study. However in the absence of an argument for a different choice for $\overline{|\dot{y}(S_y)|}$, the [1] value of 36 NM is used. This corresponds approximately to a track at 5 degrees to the nominal track.

8.6.2 The average relative vertical speed of two aircraft assigned to the same flight level, $\overline{|\dot{z}|}$, is set to the same value used in all recent safety assessments to support separation changes in the Pacific and North Atlantic, $\overline{|\dot{z}|} = 1.5$ knots.

8.7 Speed error distribution: scale parameter λ_v and truncation

8.7.1 The double exponential scale parameter λ_v is often set to a historical value of 5.82 knots. However a recent review of paired aircraft speed data [7] indicates that this value is very over-conservative for aircraft pairs in close proximity. Evidence showed that aircraft in such pairs do not have independent speeds. They are subjected to greater ATC scrutiny and any speed difference is carefully managed. The risk assessment performed here adopts the value $\lambda_v = 2.5$ knots [7]. That still provides a conservative risk estimation for aircraft in close proximity.

8.7.2 The infinite integration ranges for V_1 and V_2 in (4) were truncated to the range 480 ± 80 knots and the probability density was renormalised.

8.8 ADS-C reporting interval T

8.8.1 The standard ADS-C Periodic Contract rates appear to be 832 seconds (rounds to 14 minutes) and 2368 seconds when ADS-B is also available (rounds up to 40 minutes). Longitudinal risk is shown for a range of T.

8.9 ATC intervention buffer τ

8.9.1 Three values are used: $\tau = 4,\ 10.5$ and 13.5 minutes as explained in Tables H-4 to H-6 of [1].

8.10 Number of pairs with ATC intervention per flight hour: NP

8.10.1 As with Appendix H of [1] we set a conservative value of NP=1.

9 Lateral Risk

9.1 Calculations using equation (3) gave Table 12. Without the unspecified LLD given to EAST the risk would have been $N_{ay} = 8 \times 10^{-13}$ (fapfh). The lateral risk in all three regions is found to be well under the TLS of (5×10^{-9} fapfh).

Region	N_{ay} **(FAPFH)**
WEST	2.62×10^{-9}
NORTH	1.91×10^{-9}
EAST	1.92×10^{-9}

Table 12. Lateral risk (expected fatal accidents per flight hour) as estimated in each region for all aircraft assuming all OCA aircraft were RNP 4.

10 Longitudinal Risk

10.1 Longitudinal collision risk estimates calculated with equation (4) are illustrated for the WEST region in Figures 4 and 5. The speed distribution in both Figures extended over 480 ± 80 knots with a Double Exponential scale parameter $\lambda_v = 2.5$ knots [7].

10.2 Figure 4 was calculated using a uniform initial longitudinal separation over 50 to 75 NM. Results are shown for RNP 10 and for ONP 0.3. The latter is a better approximation to the navigational accuracy of GNSS aircraft. Both curves show risk well under the TLS (5×10^{-9} fapfh), with the ONP 0.3 aircraft having particularly low risk.

10.3 Figure 5 had initial aircraft separations in the range 30 to 55 NM. Once again risks are well below the TLS, and risk is about three orders of magnitude lower than the 50 NM cases.

10.4 Plots for NORTH and EAST regions were very similar to the WEST Figures. They were not included since their risk is slightly lower due to the smaller aircraft present.

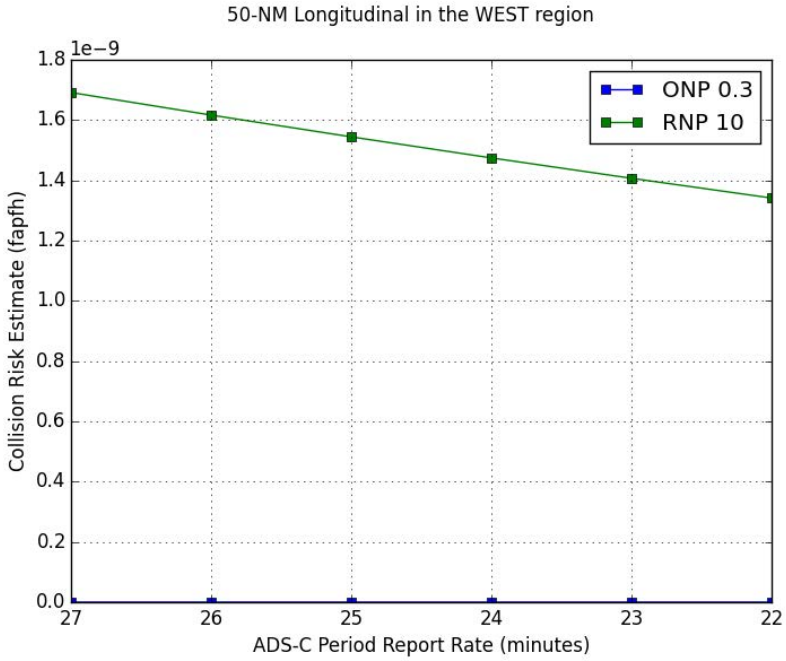

Figure 4. 50 NM longitudinal separation collision risk estimates in WEST OCA for a range of reporting time T minutes.

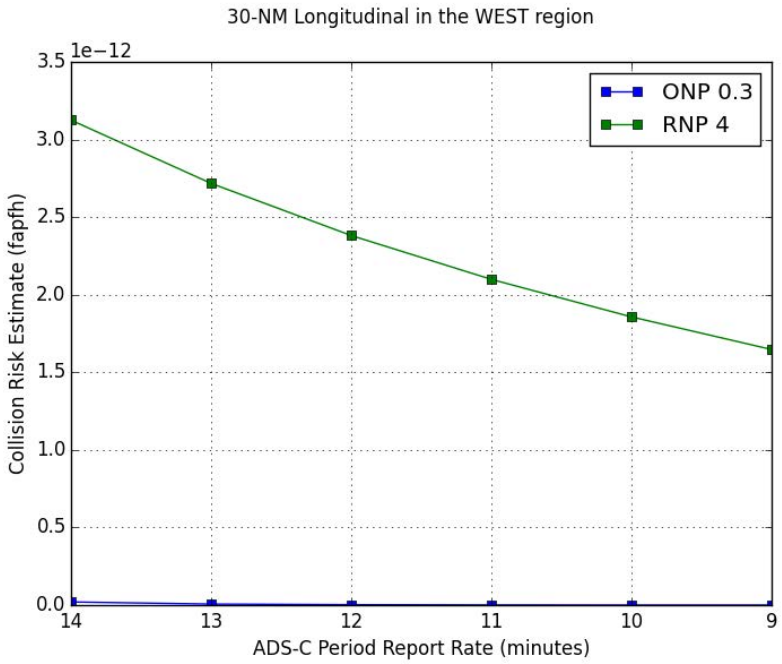

Figure 5. 30 NM longitudinal separation risk estimates in WEST OCA for a range of reporting time T minutes.

References

[1] Draft PBHSM manual, attachment to *Development of Global Guidance for Monitoring the Application of Performance-Based Horizontal Separation Minima*, SASP-WG/27-WP/20, Oklahoma City, November 2015

[2] ICAO Document 9689, *Manual on Airspace Planning Methodology for the Determination of Separation Minima*, 1st Ed, 1998

[3] ICAO Document 9869, *Manual on Required Communication Performance*, 1st Ed, 2008

[4] ICAO Document 4444 *Procedures for Air Navigation Services - Air Traffic Management*, 15th Ed, 2007

[5] ICAO Circular 319, *A Unified Framework for Collision Risk Modelling in Support of the Manual on Airspace Planning Methodology for the Determination of Separation Minima (Doc 9689)*, 2009

[6] *The Lateral Overlap Probability for a Pair of Aircraft with Unequal Normal-Double Exponential Lateral Deviation Distributions*, IP1, ICAO SASP-WG/WHL/17, Montreal, May 2010

[7] *An Overview of Position Prediction and Speed Error*, WP17, ICAO SASP-WG/28, Rejkjavik, May 2016